Vol 15 No 5, May 2006
1009-1963/2006/15(05)/1090-06

Chinese Physics

© 2006 Chin. Phys. Soc.
and IOP Publishing Ltd

Infrared active phonon modes and ionicity of single crystal $MgAl_2O_4$*

Bi Cong-Zhi(毕聪志)[a),b)], Ma Ji-Yun(马继云)[b)], Yan Jun(颜　俊)[b)], Fang Xu(方　煦)[b)], Zhao Bai-Ru(赵柏儒)[b)], Yao Duan-Zheng(姚端正)[a)], and Qiu Xiang-Gang(邱祥冈)[b)†]

[a)] *Department of Physics, Wuhan University, Wuhan 430072, China*

[b)] *National Laboratory for Superconductivity, Institute of Physics, Chinese Academy of Sciences, Beijing 100080, China*

(Received 21 November 2005; revised manuscript received 3 March 2006)

Near-normal incident infrared reflectivity spectra of (100) $MgAl_2O_4$ spinel single crystal have been measured at different temperatures in the frequency region between 50 and 6000 cm^{-1}. Eight infrared-active phonon modes are identified, which are fitted with the factorized form of the dielectric function. The dielectric property and optical conductivity of the $MgAl_2O_4$ crystal are analysed. From TO/LO splitting, the effective Szigeti charges and Born effective charges at different temperatures are calculated for studying the ionicity and the effect of polarization. Based on the relationship between the $(LO–TO)_1$ splitting, which represents the transverse and longitudinal frequencies splitting of the highest energy phonon band in the reflectivity spectrum, and the ionic-covalent parameter, the four main phonon modes are assigned. $MgAl_2O_4$ can be considered as a pure ionic crystal and its optical characters do not change with decreasing temperature, so it may be used as a suitable substrate for high-T_c superconducting thin films.

Keywords: $MgAl_2O_4$ single crystal, phonon, dielectric function, effective charges
PACC: 7830, 7820D, 6320, 7720

1. Introduction

As a kind of stable ceramic material, magnesium dialuminate oxide ($MgAl_2O_4$) may be refined from natural mineral in the earth's mantle.[1,2] Due to its many special characteristics such as high melting point, good chemical resistance, excellent mechanical strength, low electrical loss and resistance to ion bombardment at high temperatures,[3–8] it has been employed extensively in different fields, especially in high temperature and/or high pressure environment.[9–11] A lot of works have been reported on its optical properties in crystals made by various synthetic processes[12–17] and in its high-pressure form,[9] etc. Single crystal $MgAl_2O_4$ has also been used as the substrate for the growth of high-T_c superconducting thin films, which can satisfy the requirements for an ideal insulating substrate, namely, lattice matched, chemically compatible, thermal expansion matched, and undergoing no structural phase transition in the region between the film growth and the device operation temperatures.

The crystal structure of $MgAl_2O_4$ spinel is face-centred cubic (fcc), with space group Fd3m (O_h^7, No.227 in the International Tables),[18] which is often considered as a prototype compound of the AB_2O_4 family. A unit cell with composition of AB_2O_4 consists of an approximately cubic-close-packed array of 32 oxygen atoms, with one-eighth of the 64 tetrahedral holes per unit cell and one-half of the 32 octahedral holes per unit cell filled by the cations A and B. The resulting unit cell contains eight formula units of AB_2O_4, with Mg, Al and O located at 8a, 16d and 32e sites, respectively. The Mg and Al atoms occupy special positions and their separation depends only on the cubic cell parameter, a. The position of the oxygen anions is determined by an additional parameter, u. In the ideal structure with $a = 0.806$ nm, $u = 0.362$, each oxygen anion is coordinated on one side with an equilateral triangle of three Al cations, and on the other side by one Mg cation. Each Mg cation is at the centre of an oxygen tetrahedron, and each Al cation resides at the centre of a perfect oxygen octahedron. The oxygen octahedra surrounding the Al cation share edges with each other, and share corners with the oxygen tetrahedra surrounding the

*Project supported by the National Natural Science Foundation of China (Grant No 10474128) and Chinese Academy of Sciences.
†Correspondence Author. E-mail: xgqiu@aphy.iphy.ac.cn

Mg cations. However, these tetrahedra do not contact with each other.

There have been a lot of works on the vibrational modes of spinel $MgAl_2O_4$ measured by Raman and far infrared reflectivity and/or transmission spectra.[19–25] However, no conclusion can be drawn yet on the number of infrared active modes. It is of great interest to explore its infrared properties and determine its dielectric function in order to facilitate its utilization as a substrate for the growth of high-temperature superconductors. Moreover, there has rarely any report on its temperature-dependent optical response, which is important from the viewpoint of being a substrate for devices operating at low temperatures. In the present paper we report our work on the far-infrared and mid-infrared reflectivity spectra of $MgAl_2O_4$. Eight vibration modes are identified, among which four are intrinsic for its lattice structure. The frequency-dependent complex dielectric function and optical conductivity at different temperatures are obtained.

2. Experimental procedures

Single crystal of $MgAl_2O_4$ was grown by Hefei Kejing Materials Technology Co. Ltd. with Czochralski growth method. A rectangular piece (10 mm× 10 mm×0.5 mm) was cut and one-side polished with the surface parallel to the (100) plane. X-ray diffraction gave its lattice parameter $a = 0.807$ nm. Near-normal incident measurements (with the incident angle about 8°) were performed with the electric field perpendicular to the crystallographic c-axis (i.e., $E//ab$). All the reflectivity spectra were taken on a BOMEM DA8 FT-IR spectrometer in the range of 50–6000 cm^{-1} with a resolution of 4 cm^{-1}. The sample was mounted in an optical cryostat in vacuum and the temperature was varied from 300 to 10 K with an accuracy of 0.02 K. A deuterated triglycine sulfate (DTGS) pyroelectric detector was utilized in the far-infrared range of 50–700 cm^{-1}, and a liquid-nitrogen cooled mercury cadmium telluride detector was employed in the mid-infrared range of 450–6000 cm^{-1}. To obtain the absolute reflectivity, an evaporated-gold mirror was served as a reference.

3. Results and discussion

Shown in Fig.1 are the reflectivity spectra of the $MgAl_2O_4$ single crystal at different temperatures. The reflectivity of the $MgAl_2O_4$ single crystal is typical of an insulator. The sharp features in the reflectivity at low frequencies are due to the unscreened infrared-active optical phonon modes; while above the highest observed lattice vibration frequency the reflectance is flat and featureless up to the highest measured frequency. It can be seen that there are eight phonon peaks centred at about 210, 304, 431, 537, 709, 737, 823 cm^{-1}at room temperature, but they do not correspond to really active frequencies. The following model fitting will give their parameters. On the other hand, the reflectivity within the reststrahlen bands increases slightly with decreasing temperature. It is due to the fact that anharmonic thermal motion would become weaker with decreasing T so that the oscillation strength of the modes enhances, which is in agreement with the insulating character of $MgAl_2O_4$. From 300 to 20 K, $MgAl_2O_4$ undergoes no structural transition. Hence the phonons are only slightly influenced by temperature.

The mode frequencies are obtained from a damped harmonic oscillator fit to the reflectance spectra with a complex dielectric function $\varepsilon(\omega)$ in the factorized form (generalized Lyddane–Sachs–Teller relation)[26–29]

$$\begin{aligned}\varepsilon(\omega) =&\varepsilon_1(\omega) + \mathrm{i}\varepsilon_2(\omega)\\ =&\varepsilon_\infty \prod_j^N \frac{\omega_{j\mathrm{LO}}^2 - \omega^2 + \mathrm{i}\omega\gamma_{j\mathrm{LO}}}{\omega_{j\mathrm{TO}}^2 - \omega^2 + \mathrm{i}\omega\gamma_{j\mathrm{TO}}}\,, \end{aligned} \tag{1}$$

where ε_∞ is the high-frequency dielectric constant, $\omega_{j\mathrm{TO}}$ and $\omega_{j\mathrm{LO}}$ are the transverse and longitudinal eigenfrequencies of the jth optical phonon mode, and $\gamma_{j\mathrm{TO}}$ and $\gamma_{j\mathrm{LO}}$ the corresponding transverse and longitudinal damping constants. Using this dielectric function, all the reflectivity spectra were fitted with the well-known Fresnel formula:[30]

$$R(\omega) = \left|\frac{\sqrt{\varepsilon(\omega)} - 1}{\sqrt{\varepsilon(\omega)} + 1}\right|^2 . \tag{2}$$

Based on Eqs.(1) and (2), a fit of R(ω) to the observed reflectivity spectra can be obtained with a proper choice of the model parameters $\omega_{j\mathrm{TO}}$, $\omega_{j\mathrm{LO}}$, $\gamma_{j\mathrm{TO}}$, $\gamma_{j\mathrm{LO}}$ and ε_∞. Adjustment of the parameters is made by trial and error fitting of Eq.(2) to the experimental spectra. This method yields not only $\varepsilon(\omega)$ but also the model parameters which characterize the infrared active phonons.

Shown in Fig.2 are the fitting results, by assuming a value of $\varepsilon_\infty = 2.96$. The dot-dashed line indicates the experimental FIR reflectivity spectrum and the solid line is the fitting result. Excellent agreement between the fitting and the experimental results

is obtained. The fitting parameters at the two representative temperatures 300 and 20 K are listed in Table 1.

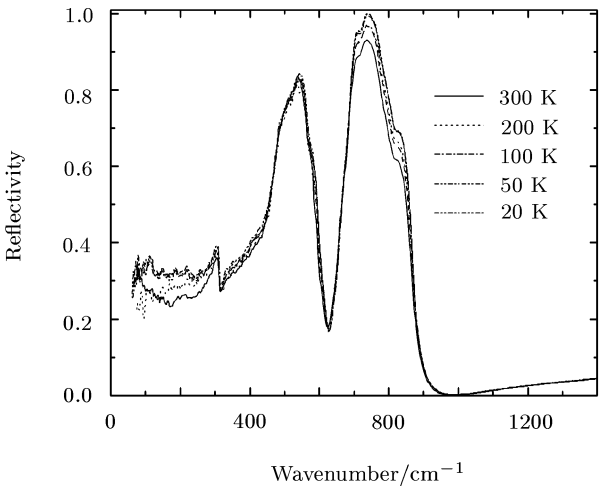


Fig.1. Experimental far-infrared reflectivity spectra of $MgAl_2O_4$ crystal at various temperatures.

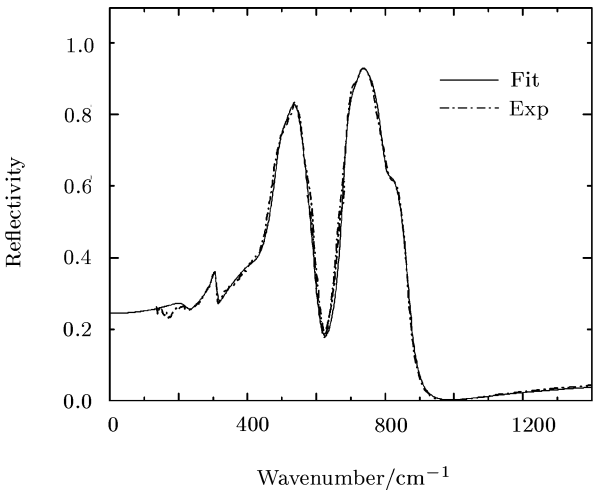


Fig.2. The experimental spectrum of the synthetic sample of $MgAl_2O_4$ from 50 to 1400 cm^{-1} at 300 K (dot-dashed line). The solid line denotes the fitting curve with the LST relation.

Table 1. The fitting parameters of eight oscillators including transverse modes, longitudinal modes and their damping factors at 300 and 20K. All units are in cm^{-1}.

300 K				20 K			
$\Omega_{j\mathrm{TO}}$	$\gamma_{j\mathrm{TO}}$	$\Omega_{j\mathrm{LO}}$	$\gamma_{j\mathrm{LO}}$	$\Omega_{j\mathrm{TO}}$	$\gamma_{j\mathrm{TO}}$	$\Omega_{j\mathrm{LO}}$	$\gamma_{j\mathrm{LO}}$
224	50	227	45	218	27	219	38
306	16	310	18	305	15	310	18
415	99	430	90	410	100	435	115
486	30	606	60	482	24	606	55
528	54	536	68	530	49	532	73
678	22	870	38	679	17	870	32
722	36	722	38	723	37	722	37
803	49	798	45	803	47	799	45

From group theoretical analysis,[31] it is well known that the compounds with the normal spinel structure symmetry with two chemical formulas in a primitive unit cell should have the Brillouin zone centre modes at the Γ point with

$$\Gamma(k=0) = A_{1\mathrm{g}}(R) + E_{\mathrm{g}}(R) + 3T_{2\mathrm{g}}(R) + 4T_{1\mathrm{u}}(\mathrm{IR}) + T_{1\mathrm{g}} + 2A_{2\mathrm{u}} + 2E_{\mathrm{u}} + 2T_{2\mathrm{u}}\,.$$

Among these 16 normal modes, $A_{1\mathrm{g}}$, E_{g} and $T_{2\mathrm{g}}$ are Raman active and the total number is five, while four $T_{1\mathrm{u}}$ are all infrared active. Recently, first-principles calculation of the phonon spectrum performed by de Wijs *et al*[32] gives four transverse optic modes at 311, 512, 588, 698 cm^{-1}, the corresponding longitudinal optic modes are at 319, 580, 638, 866 cm^{-1}, respectively. The first and the last modes match our results well, although there are some discrepancies for the second and third. Furthermore, the modes at 311 and 698 cm^{-1} have also been obtained in experiment by Chopelas and Hofmeister,[33] Hill *et al*[34] Striefler and Boldish.[35] The main features of our reflectivity spectra agree with those of O'Horo *et al*[36] who observed four modes at 305, 428, 485, 670 cm^{-1}. Here we assign these four modes as the main structural modes that dominate the features in the reflectivity spectrum. The number is consistent with the result from the group theoretical analysis. The other four modes may originate from the difference between natural and synthetic $MgAl_2O_4$. Based on the above consideration, we use a synthetic sample that is highly prone to com-

plicated cation disorder that is induced mainly by the cation exchange taking place at the two tetrahedral Mg and octahedral Al sites. Since Mg and Al cations may take variable occupations, there exist four defective modes in the measured spectra. It is worth noting that the 722 cm^{-1} mode has never been reported before in the infrared measurements, except a similar mode in the Raman measurements.[37,38] We think that it may result from the AlO_4 tetrahedron: i.e., from the cation disorder. The AlO_4 forms through the exchange of an Al atom and a Mg atom, then the calculations with AlO_4 tetrahedron display two breathing modes due to different oscillating AlO_4 couplings. The two modes are at 722 cm^{-1} and 757 cm^{-1} respectively, consistent with the modes at 723 cm^{-1}observed in this work. In order to identify which mode has its relation with structural defects, we have annealed the crystal at 800°C under an oxygen atmosphere for 10 h. Then the reflectivity spectra were measured again at room temperature. The mode at 224 cm^{-1} disappeared, which suggests that this may be related with defects such as oxygen vacancies inside the crystal. But the other three defective modes do not change during annealing. It is necessary to carry out further investigations in order to clarify their origin.

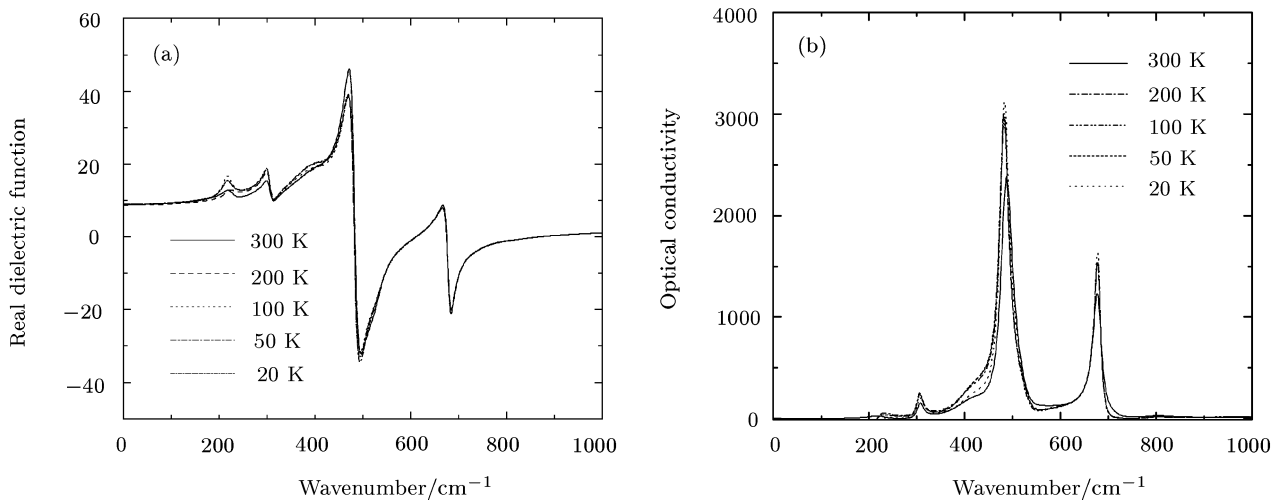


Fig.3. The real parts of the dielectric function (a) and optical conductivity (b) for temperatures between 20 and 300 K from 0 to 1000 cm^{-1}.

Shown in Fig.3(a) is the real part of the dielectric function vs ω at different temperatures. The real part of the frequency-dependent optical conductivity $\sigma_1(\omega)$ can be obtained according to $\sigma_1(\omega) = (\omega/4\pi)\varepsilon_2(\omega)$. The spectrum shown in Fig.3(b) is dominated by the four-peak structures due to optical phonon absorption, and no free carrier contribution can be observed. This agrees well with the fact that $MgAl_2O_4$ is a good insulator.

In the approximation of zero phonon, one can simply obtain the LST relation from Eq.(1), which connects the static optical permittivities ε_0 and the high-frequency optical permittivities ε_∞ with transverse and longitudinal phonon frequencies:

$$\frac{\varepsilon_0}{\varepsilon_\infty} = \prod_i \frac{\Omega_{i\mathrm{LO}}^2}{\Omega_{i\mathrm{TO}}^2}. \qquad (3)$$

LST relationship also provides an effective examination on the parameters used to fit the vibration spectra. With $\varepsilon_\infty = 2.96$ and $\varepsilon_0 = 8.42$,[39] we obtain 2.84 for the left-hand side of Eq.(3). On the other hand, by inserting the parameters listed in Table 1, we have a value of 2.94 for the right-hand side, in accord with what is required by the LST relation.

Effective ionic charges (Szigeti charges e_S^*/e) and Born effective charges calculated from TO/LO splittings of the phonon modes have been used to study the bonding, especially the ionicity and the effect of polarization, of compounds. If the normalized splitting is denoted by S, the effective charge could be expressed as

$$\frac{Ze^*}{e} = S^{1/2}.$$

For a normal material with AB_2O_4 structure, the relationship between the normalized TO/LO splitting

and the effective charge is given by[40]

$$4\pi^2c^2\sum_j \omega_{\mathrm{LO}j}^2 - \omega_{\mathrm{TO}j}^2 = \frac{4\pi}{V}e^2Z\Big[\frac{n_{\mathrm{A}}(Ze^*/e)_{\mathrm{A}}^2}{m_{\mathrm{A}}} + \frac{n_{\mathrm{B}}(Ze^*/e)_{\mathrm{B}}^2}{m_{\mathrm{B}}} + \frac{n_0(Ze^*/e)_0^2}{m_0}\Big], \quad (4)$$

where c is the velocity of light, and V the volume of the unit cell; e and Z are elementary charge and number of formula units in the cell respectively, n_{A}, n_{B}, n_O represent stoichiometric coefficients, and m_{A}, m_{B}, m_O atomic masses. The TO and LO phonon frequencies of the spinel $MgAl_2O_4$ under investigation are obtained from the fitting results by LST relation as listed in Table 1. With the assumption that the charge of the bivalent metal is equal to 2/3 that of the trivalent ones, i.e., $(Ze^*/e)_{\mathrm{A}} = (2/3)(Ze^*/e)_{\mathrm{B}} = -(Ze^*/e)_{\mathrm{O}}$, it is possible to calculate the effective charges from TO/LO splittings of the phonon modes at different temperatures. On the other hand, Szigeti charge is defined by $e_{\mathrm{S}}^*/e = (3e_{\mathrm{B}}^*/e)/(\varepsilon_\infty + 2) = \sqrt{S\varepsilon_\infty}/(\varepsilon_\infty + 2)$, where e_{B}^*/e denotes as the Born effective charge. Combining all the above formulas, we can calculate the Szigeti charges and Born effective charges. A plot of Szigeti charges versus temperature is shown in Fig.4. For comparison, the temperature-dependent static dielectric constant curve is also included in the plot. Our result gives the magnesium's Szigeti charge e_{S}^*/e of 1.184, and aluminium's Szigeti charge e_{S}^*/e of 1.776, which means that nearly $1.184e$ per magnesium atom is transferred on average to oxygen atom. With decreasing temperature, the value slightly increases and reaches $1.193e$ at 20 K, which can be considered as the result from reduced thermal fluctuation. For Born effective charges, the value is 1.97 for Mg cation and 2.95 for Al cation, which are a little smaller than those of the formal charges (Mg:+2, Al:+3). So good agreement suggests that there is little hybridization between cations and O anions, then $MgAl_2O_4$ is almost pure ionic crystal. But the calculation contains the contributions of all modes observed. In order to evaluate the effect of the defects and cation disorder on ionicity, we calculate Born effective charges again with the four main structure modes defined above and obtain the values of 1.98 and 2.97, respectively. It may be reasonably concluded that the presence of the disorder and defects breaks the symmetry of the perfect tetrahedral and octahedral lattices, induces the increase of the hybridization and decreases the ionicity. However, the effect is weak and the crystal still can be regarded as pure ionic crystal. The measured Born effective charges are close to the values theoretically calculated by Xu and Ching.[41] The small discrepancy between them may be due to the assumption between the bivalent and trivalent metals and a lack of precision in their frequency determination.

On the other hand, the $(\mathrm{LO\text{-}TO})_1$ splitting of the high-energy band serves as a criterion for the ionic character, which can be influenced by cation disorders. The $(\mathrm{LO\text{-}TO})_1$ value (about 194 cm^{-1}) obtained from the fitting results is related to a new electronegativity scale[42] and the ionic radii scale. The splitting is mainly determined by the octahedral trivalent cations. Its temperature independence suggests that the cation disorder does not change with temperature. From the relationship between TO/LO splitting and the ionic-covalent parameter,[42,43] isomorphic replacements of tetrahedral and octahedral cations in solid solutions and the investigation of isotopic substitutions for some spinels,[44,21] we conclude that among the four dominant phonon peaks, the two high-frequency modes are essentially related to vibrations of the lattice of octahedral groups. Their frequencies are mainly determined by the bonding force between the trivalent cation and the oxygen anion. The two low-frequency bands correspond to complex vibrations involving the simultaneous participation of the tetrahedral and octahedral cations.

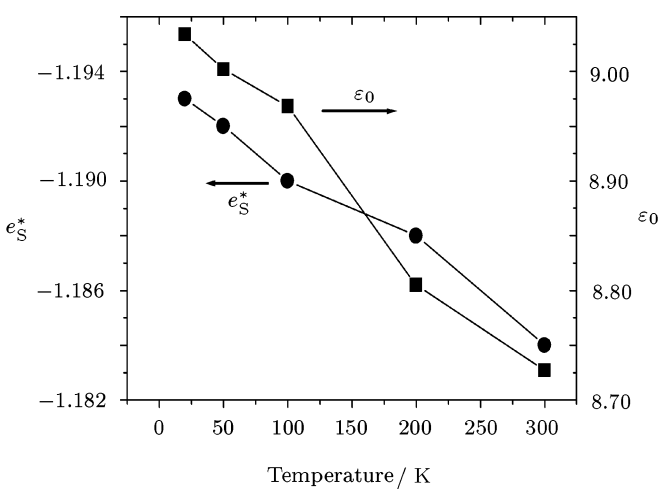


Fig.4. The temperature dependence of Szigeti effective charge and static optical permittivities in $MgAl_2O_4$. The dots represent the deduced values at various temperatures.

4. Conclusion

In summary, the infrared reflectivity spectra of the synthetic spinel $MgAl_2O_4$ have been fitted us-

ing LST relation with excellent agreement at different temperatures. Four of the eight-phonon modes are attributed to the vibrational modes of the main structure of the crystal, which consists with the experimental results previously reported. The other four modes are considered as the defective or disorder modes of the synthetic sample. Furthermore, a mode at 722 cm^{-1} was observed which is speculated to arise from the distortion of AlO_4 tetrahedron induced by cations exchange. The vibration mode at 224 cm^{-1} is associated with the defects inside the crystal. The charge transfer between cations and oxygen atoms has been determined in terms of effective Szigeti charges. Evidence is found that nearly 1.184e per magnesium atom is transferred on average to oxygen atom in $MgAl_2O_4$. Born effective charges suggest it to be a pure ionic crystal. From the relationship between $(LO–TO)_1$ splitting and the ionic-covalent parameter, a simple mode assignment is given. The low dielectric constant and temperature-independent optical character make the compound a suitable substrate for microwave devices operating at low temperatures, such as, the microwave filter made up of high-T_c superconducting thin films.

References

[1] Ravenstein E G 1891 *Nature* **44** 423
[2] Ringwood A E and Major A 1970 *Phys. Earth Planet. Inter.* **3** 89
[3] White G S, Jones R V and Crawford J H 1982 *J. Appl. Phys.* **53** 265
[4] Bakkar W and Lindsay J G 1967 *Am. Ceram. Soc. Bull.* **46** 1094
[5] Roy D W and Hastert J L 1983 *Ceram. Eng. Sci. Proc.* **4** 502
[6] Gutierrez-Campos D, Diaz J I and Rodriguez R M 1999 *Ceramica* **45** 93
[7] Jones W and Miles L J 1971 *Proc. Br. Ceram. Soc.* **19** 161
[8] Leger J M, Haines J, Schmidt M, Petitet J P, Pereira A S and daJornada J A H 1996 *Nature* **383** 401
[9] Irifune T, Fujino K and Ohtani E 1991 *Nature* **349** 409
[10] Bratton R J 1974 *J. Am. Ceram. Soc.* **57** 283
[11] Panz K, Stroh N and Riedel R 1998 *Key Eng. Mater* **150** 135
[12] Ishimaru M, Afanasyev-Charkin I V and Sickafus K E 2000 *Appl. Phys. Lett.* **76** 2556
[13] Reveron H, Gutierrez-Campos D, Rodriguez R M and Bonassin J C 2002 *Mater. Lett.* **56** 97
[14] Park H C, Lee Y B, Oh K D and Riley F L 1997 *J. Mater. Sci. Lett.* **16** 1841
[15] Salmones J, Galicia J A, Wang J A, Valenzuela M A and Aguilar-Rios G 2000 *J. Mater. Sci. Lett.* **19** 1033
[16] Kong L B, Ma J and Huang H 2002 *Mater. Lett.* **56** 238
[17] Varnier O, Hovnanian N, Larbot A, Bergez P, Cot L and Charpin J 1994 *Mater. Res. Bull.* **29** 479
[18] Grimes N W, Thompson P and Kay H F 1993 *Proc. R. Soc. Lond.* A **386** 333
[19] Fraas L M, Moore J E and Salzberg J B 1973 *J. Chem. Phys.* **58** 3585
[20] Ohwaki T and Onishi T 1999 *Jpn. J. Appl. Phys.* **38** L1191
[21] Preudhomme J and Tarte P 1991 *Spectrochim. Acta.* A **27** 1817
[22] Slack G A 1964 *J. Am. Ceram. Soc.* **134A** 1268
[23] Grimes N W, O'Connor P J and Thompson P 1978 *J. Phys.* C: *Solid State Phys.* **11** L505
[24] Thompson P and Grimes N W 1974 *Solid St. Commun.* **25** 609
[25] Yang T T, Horng H E, Yang H C, Jang I J, Kang W N and Yom S S 1994 *Physica* C **235-240** 1445
[26] Massa N E, Campa J and Rasines I 1995 *Phys. Rev.* B **57** 15920
[27] Homes C C, Ziaei M, Clayman B P, Irwin J C and Franck J P 1995 *Phys. Rev.* B **51** 3140
[28] Homes C C, Li Q, Fournier P and Greene R L 2002 *Phys. Rev.* B **66** 144511
[29] Bi C Z, Ma J Y, Zhao B R, Tang Z, Yin D, Li C Z, Yao D Z, Shi J and Qiu X G 2005 *J. Phys.: Condens. Matter* **17** 5225.
[30] Shen X C and Chu J H 1983 *Acta Phys. Sin.* **34** 56 (in chinese)
[31] White W B and De Angelis B A 1967 *Spectrochim. Acta* **23A** 985
[32] de Wijs G A, Gang C M, Kresse G and de With G 2002 *Phys. Rev.* B **65** 94305
[33] Chopelas A and Hofmeister A M 1991 *Phys. Chem. Miner.* **18** 279
[34] Hill R J, Craig J R and Gibbs G V 1979 *Phys. Chem. Miner.* **4** 317
[35] Striefler M E and Boldish S I 1978 *J. Phys.* C: *Solid State Phys.* **11** L237
[36] O'Horo M P, Frisillo A L and White W B 1973 *J. Phys. Chem. Solids.* **34** 23
[37] Ishii M, Hiraishi J and Yamanaka T 1982 *Phys. Chem. Minerals.* **8** 64
[38] Cynn H, Sharma S K, Cooney T F and Nicol M 1992 *Phys. Rev.* B **45** 500
[39] Wang C C and Zanzucchi P J 1971 *J. Electrochem. Soc.* **118** 586
[40] Lutz H D, Waschenbach G, Kliche G and Haeuseler H 1983 *J. Solid State Chem.* **48** 196
[41] Xu Yong-Nian and Ching W Y 1991 *Phys. Rev.* B **43** 4461
[42] Lenglet M and Hochu F 1997 *Mater. Res. Bull.* **32** 863
[43] Portier J, Campet G, Etourneau J and Tanguy B 1994 *J. Alloy Comp.* **209** 285
[44] Preudhomme J and Tarte P 1991 *Spectrochim. Acta* A **27** 845